ACADEMIA ROMÂNĂ
Revue Roumaine de Chimie
http://web.icf.ro/rrch/

Rev. Roum. Chim.,
2018, *63*(7-8), 685-695

Dedicated to Professor Bogdan C. Simionescu
on the occasion of his 70th anniversary

REUSABLE BIOCATALYST BY PEPSIN IMMOBILIZATION ON FUNCTIONALIZED MAGNETITE NANOPARTICLES

Ioan-Andrei DASCĂLU,[a] Leonard IGNAT,[a] Mauruşa-Elena IGNAT,[a*] Florica DOROFTEI[a], Kalim BELHACENE,[b] Renato FROIDEVAUX[b] and Mariana PINTEALĂ[a]

[a] "Petru Poni" Institute of Macromolecular Chemistry Iaşi, Centre of Advanced Research in Bionanoconjugates and Biopolymers, 41A Ghica Voda Alley, Iaşi 700487, Roumania
[b] Institut Charles Viollette - EA 7394, Université Lille Nord de France, F-59000 Lille, France

Received August 1, 2017

Magnetite nanoparticles (MNp) have been prepared as appropriate supports for pepsin loading with the aim to obtain active and reusable biocatalytical constructs. Physical adsorption on amino-functionalized MNp and covalent immobilization on glutaraldehyde pre-activated MNp were comparatively tested as viable methods for the immobilization of pepsin extracted from porcine gastric mucosa. The chemical composition, size and morphology of resulting pepsin-magnetite nanostructures were determined. Optimum results have been obtained for pepsin immobilized by physical adsorption in acid media, when a total amount of 2 mg pepsin was loaded on each mg of MNp. Furthermore, the MNp-immobilized pepsin was able to catalyze several cycles of hemoglobin hydrolysis after successive recovery through magnetic separation.

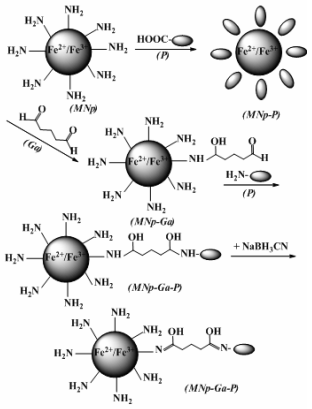

INTRODUCTION

Enzymes are frequently used under an insolubilized form due to the improved stability and recovery, relative simple recycling procedures and facile processing.[1] Common procedures involve encapsulation, crosslinking and attachment of enzymes to prefabricated carriers mainly by covalent and adsorptive binding.[2,3] Among these immobilization techniques, adsorption requires the establishing of electrostatic or hydrophobic interactions between support and enzyme, is relative simple, affordable, allows the retaining of a high catalytic activity and reuse of supports after the inactivation of immobilized biocatalyst.[4,5] Other leading technique, the covalent binding, involves an irreversible coupling of enzymes to a suitable carrier, which is the most stable form of immobilization. A wide range of chemical binding mechanisms and insoluble supporting materials may be used, but covalent binding is usually a more complex and expensive technique than adsorption.[6,7] It may also lead to losses in enzyme activity due to the lower macromolecular flexibility as result of multi-point attachment.[8]

Regarding the supporting materials, an important applicative advantage is given by their reusability potential. In this context, the magnetic

* Corresponding author: mignat@icmpp.ro

field extraction applied to various magnetic particles has received a great interest in the latest decades due to the very simple and cost effective separation from reaction media as well as due to the inherent high potential for multiple uses.[9,10] Moreover, their size, shape and surface functionality can be tailored to acquire appropriate capabilities for the selective binding and transport of different bioactive or chemical compounds.[11]

The magnetic particles are used for a long time for enzyme immobilization.[12] They are generally comprised from a core with appropriate magnetic, physical and chemical properties like magnetite or other magnetic iron oxides, and an organic shell able to ensure the physico-chemical resistance of the core. The external shell should also provide the chemical functionalities needed for enzyme binding and exhibit the characteristics required by a given application.[13,14] The chemical composition of the grafted shell dictates the surface properties, while the size, shape and magnetic properties highly depend on the reaction conditions chosen for core synthesis, like the initial Fe^{2+}/Fe^{3+} molar ratio, the successful avoidance of oxidizing species, stirring speed, pH, ionic strength and temperature.[15-20]

Due to their advantageous properties, and especially to the facile separation of enzyme-support constructs from reaction media, various core-shell type magnetic nanoparticles (MNp) have been widely used for enzyme immobilization.[21-23] Nevertheless, pepsin is a rarely immobilized enzyme due to its high sensibility to the available binding methods. Pepsin, an aspartic peptidase, is one of the three main proteolytic enzymes of the digestive system, along with chymotrypsin and trypsin, and is especially efficient in the digestion of proteins to peptides and amino acids at very low pH values (pH 1-3). The hydrolysis of peptide bonds between hydrophobic amino acids makes it very important in processes like degradation, separation, analysis and identification of proteins and peptides, biocatalysis, biomedicine, food manufacturing and chromatography.[24-26]

Unfortunately, the pepsin requirements for a very low pH usually interfere with immobilization procedures drastically narrow the type of potential effective supports and preparation techniques. Despite some promising results obtained with either physical or chemical insolubilized pepsin on supports like solid polymers,[27,28] alumina[29] and gold nanoparticles,[30] there is a high demand to extend and improve the range of such biocatalysts. Since the reports on pepsin immobilized on MNp are even scarcer,[31-33] we have designed and prepared in the present study core-shell type MNp by using the co-precipitation technique in alkaline media, followed by *in situ* stabilization with citric acid and functionalization with a silane shell.[34] Part of the resulted MNp was also modified at surface with pending amino groups prior to pepsin binding. All obtained core-shell MNp were furthermore evaluated as potential supports for pepsin immobilization, aiming to add new feasible supports and procedures to the currently low number of potential choices.

RESULTS AND DISCUSSION

Characterization of MNp-CA, MNp-APS, MNp-P and MNp-Ga-P nanoparticles

The structure and functionality of each intermediate product were monitored during the preparation of final biocatalysts by recording the corresponding infrared spectra. In the case of nanoparticles prepared through co-precipitation and covered *in situ* with citric acid (MNp-CA; Figure 1), the presence of magnetite[35] was supported by the intense absorbance observed at 586 cm^{-1}, accompanied by a discreet shoulder at 700 cm^{-1}. The intermediate shoulder from 632 cm^{-1} is attributed to the maghemite (γ-Fe_2O_3), [36] which likely forms during the sample drying for analysis. The presence of citric acid on the nanoparticle surface was confirmed by the shifting of carbonyl peak from approximately 1720 cm^{-1} to 1620 cm^{-1}. This shift strongly indicates a conversion of carboxylic groups to carboxylates due to the interactions established between the acid and inorganic surfaces.[37]

In the case of magnetite particles covered with (3-aminopropyl)triethoxysilane (APTES), MNp-APS (Figure 1) the absorption band observed at 1008-1124 cm^{-1} was attributed to the Si-O bonds,[38] whereas the absorbance from 2924 cm^{-1} was assigned to the methylene group of pendant (3-aminopropyl) silane residues from the silane shell of nanoparticles. As expected, the absorption region assigned to the magnetite core (580-700 cm^{-1}) remains relatively unchanged as compared with the MNp-CA samples, showing that silane shell ensures an appropriate resistance to the inorganic core in the acidic environment required by pepsin. Furthermore, the successful immobilization of enzyme on MNp-APS

particles is certified by the appearance of absorption bands characteristic for amidic groups (Figure 1), which are visible in both samples (MNp adsorbed pepsin, MNp-P; respective glutaraldehyde-linked pepsin, MNp-Ga-P) at 1640 cm^{-1} (amide I) and 1530 cm^{-1} (amide II).[39]

The successive modification of MNp surface with citric acid (CA), APTES and pepsin was evaluated after each preparative step by monitoring the variation of C, N, and Si content through energy-dispersive X-ray (EDX) analysis. Due to the limitations of classical EDX analysis for heterogeneous materials with non-uniform surfaces, data obtained have been examined only from the qualitative point of view, and not as absolute values. The successful development of MNp-CA was reflected by the readings obtained for elemental carbon, while that of MNp-APS was confirmed by the appearance of nitrogen and silicon contents (Table 1). Meantime, since APTES also introduces some structural carbon in nanoparticles, the carbon content in MNp-APS is only slightly lessened compared with the MNp-CA precursor. It was also found that the compositional variation of the MNp-APS samples taken after 24 h and 48 h of reaction is negligible; thus the silicone shell was considered as completed after 24 h and this reaction time was set for all MNp-APS supports. The increase in carbon and nitrogen for pepsin loaded supports (MNp-P and MNp-Ga-P), accompanied with a reduction in overall silica percentage, confirms that physical and covalent immobilization have been both effective. Moreover, the higher silica percent obtained for MNp-Ga-P as compared with MNp-P, together with a lower content in carbon and nitrogen, strongly hints to a higher amount of pepsin immobilized by adsorption than covalent binding.

From the morphological point of view, both citrate and silane covered MNp have roughly 15-20 nm in diameter and a relative spherical shape (Figure 2). Transmission electron microscopy (TEM) images also show a relative narrow dimensional polydispersity for MNp-CA (Figure 2a) and a discrete shell on the surface of the MNp-APS (Figure 2b) that results from the successful covering of the magnetic inorganic core with oligomeric silane functional shells.

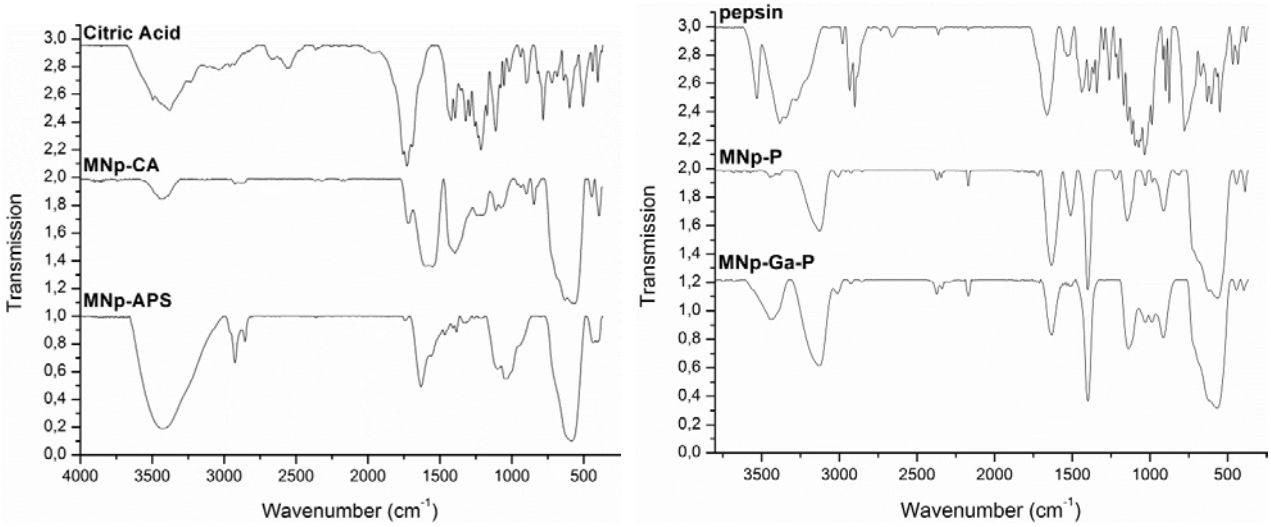

Fig. 1 – The FT-IR spectra of citric acid, MNp-CA and MNp-APS (left); pepsin, MNp-P and MNp-Ga-P (right).

Table 1

EDX analysis of pepsin and all MNp samples taken before and after pepsin loading

Element	MNp-CA wt%	MNp-APS wt%	MNp-P wt%	MNp-Ga-P wt%	Pepsin wt%
C	10.51	9.53	24.09	23.585	61.02
N	-	5.36	7.54	5.81	12.18
O	47.70	49.55	40.52	43.125	21.87
Si	-	2.62	0.48	1.325	-
P	-	-	0.10	0.75	0.80
S	-	-	0.92	0.095	0.65
Cl	-	-	1.29	0.105	3.47
Fe	41.79	32.94	25.12	25.2	-

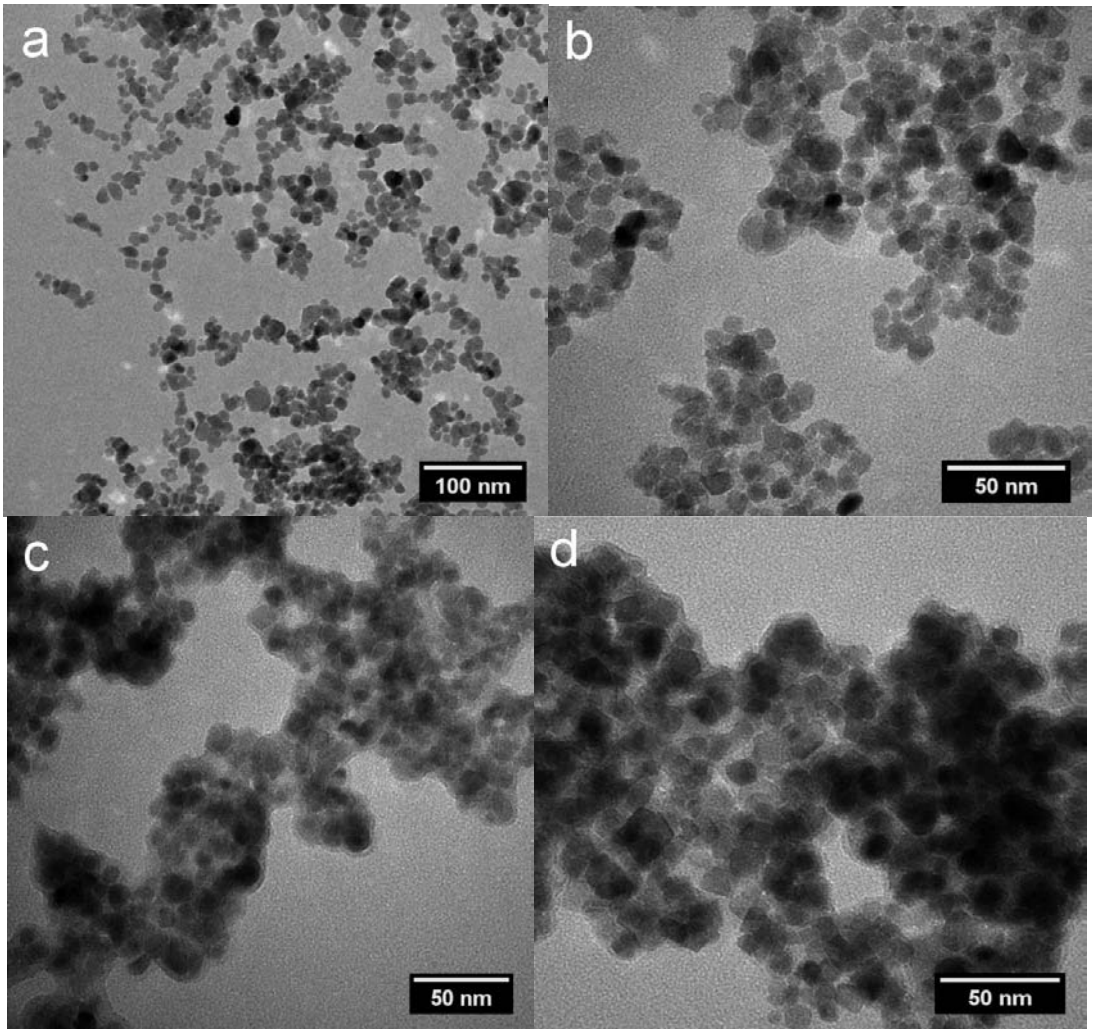

Fig. 2 – TEM images of MNp-CA (a), MNp-APS (b), MNp-P (c) and MNp-Ga-P (d).

As shown in the TEM images of MNp-P (Figure 2c) and MNp-Ga-P (Figure 2d), large clusters of particles are frequently held together by discrete shells of lower contrast attributed to the silane cover and loaded pepsin. This clustering effect is more pronounced in the case of covalent immobilization.

The dimensional evaluation using dynamic light scattering analysis (DLS) (Table 2) has supplementary confirmed the effective grafting of functional silane shell as shown by the rise of mean particle diameter from 29.7 nm in the case of MNp-CA to 87.6 nm for MNp-APS analogues. It was determined in addition that pepsin immobilization on MNp-APS particles by physical interactions (MNp-P) or covalent bonding through a glutaraldehyde spacer (MNp-GA-P) produces large clusters of approximately 1300 nm, in agreement with agglomerations observed in TEM images. In terms of colloidal stability, the zeta potential measurements (-32.97 mV) confirm the stability of MNp-CA. After the ligand exchange reaction with APTES the zeta potential becomes +36.61 mV, which also reflects the particle stability, the positive value being determined by the insertion of amino groups. However, the immobilization of pepsin was accompanied by a shift towards negative values of -12.87 mV in the case of MNp-P and -5.04 mV for MNp-Ga-P, which may be attributed to a higher exposure of aspartic and glutamic amino acid residues from the enzyme primary structure.[40] Since lower zeta potential values translate into a lower surface charge,[41] weaker electrostatic repulsions and stronger hydrophobic interactions, the individual particles tend to aggregate in relative stable, loosely self-associated supramolecular architectures with lower densities. This behavior was observed in the case of both MNp-P and MNp-Ga-P, which shows associations of remarkable similar medium sizes. Nevertheless, the significantly lower zeta potential value of MNp-Ga-P suggests different morphologies of the outer shells made from immobilised pepsin macromolecules.

Table 2

DLS size and zeta potential of MNp samples taken before and after pepsin loading

Sample	Size (nm)	Zeta potential (mV)
MNp-CA	29.7 ± 6.1	-32.97
MNp-APS	87.6 ± 22.1	+36.61
MNp-P	1302 ± 63.5	-12.87
MNp-Ga-P	1293 ± 71.8	-5.04

Table 3

Released 4-NBA values and the calculated number of NH_2 groups

MNp-APS (mg)	A (267nm)	4-NBA (µg/3mL)	4-NBA (µmoles)	NH_2 groups (No.)	NH_2 groups (No./mg)
25	0.0752	1260.241	8.339	5.02194E+18	2.01E+17
50	0.1503	3045.971	20.156	1.21379E+19	2.43E+17
75	0.1853	3878.203	25.663	1.54543E+19	2.06E+17
100	0.2204	4712.814	31.186	1.87802E+19	1.88E+17

Table 4

Pepsin loading on magnetic nanoparticles in neutral and acidic media

Samples	aqueous media (pH 6.0)			acidic media (pH 2.0)		
	residual free pepsin (mg/mL)	loaded pepsin (mg/mg)	free pepsin activity (%)	residual free pepsin (mg/mL)	loaded pepsin (mg/mg)	free pepsin activity (%)
Free pepsin	3	-	100	3	-	100
MNp-P	2.287	0.083	75.17	0.941	0.240	54.12
MNp-Ga-P	2.578	0.0892	74.5	1.546	0.169	68.44

Quantification of amino groups on the surface of MNp-APS

Prior to the immobilization of pepsin, the nanometric support was evaluated in order to establish the number of amino groups available for direct or assisted interaction with the biocatalyst. The quantification of amino groups was achieved using an adapted protocol,[42,43] which is based on the formation of a Schiff base between them and the aldehyde group of 4-nitrobenzaldehyde (4-NBA). This quantification step provides an insight on the interaction mechanisms that may occur between the biocatalyst and functional magnetic nanoparticles, as well as on the available immobilization strategies for optimal loading. Results obtained are summarized in Table 3 and indicate that a medium number of about 2.095E+17 NH_2 groups per 1 mg of MNp-APS are available for interactions on the surface of APTES covered nanoparticles.

Pepsin loading and activity

In general the processes of enzyme immobilization, besides the specific technique involved, could be largely influenced by several factors related to the reaction medium, time, ratios and absolute amounts of enzyme and support. In the case of pepsin a major difficulty in finding an appropriate support also resides in the need for a very low working pH (1-3) and low temperatures[24] to prevent its denaturation and inactivation. Since our preliminary tests showed that the MNp supports are stable in 0.01 M HCl solutions (pH 2.0), all experiments regarding the pepsin loading were carried out at pH 2.0 and 4ºC to avoid as much as possible any enzyme denaturation prior to immobilization. Moreover, the load amounts obtained at pH 2.0 after 24 h of incubation for both adsorption and covalent bonding of pepsin have been far better than those acquired in non-acidified media (Table 4).

The use of a 0.01 M HCl reaction medium not only provided a proper environment for pepsin, but also enhanced its stability in solution and ensured a better protonation of its functional groups which in turn favor the interactions with colloidal nano-supports. The physical interactions were particularly enhanced, as reflected by an approximately three fold increase in the amount of pepsin loaded by adsorption on amino-functionalized nanoparticles. Covalent binding efficiency has been also improved, but to a lower extent, data obtained showing nearly double amounts of load in acidic media. It was observed

that increasing the incubation time up to 48 h translates in similar or just very slight supplementary loads. In addition, it was found that increasing the amount of support from 1.25 to 2.5 and 5 mg/mL determined a significant drop in the amount of immobilized pepsin. Such phenomenon could be determined by the increased intensity of the magnetic field, enhanced electrostatic repulsions, mechanical collisions and hindrance.[44,45] As a result, all further studies were performed by incubation of pepsin in acidic environments (pH 2.0) containing 1.25 mg/mL magnetic nanoparticles, at 4ºC and 24 hours.

Pepsin concentrations of up to 6 mg/mL have been tested in these experimental conditions for adsorptive immobilizations. Significant loads were obtained for concentrations higher than 2 mg/mL, associated with continuous growths in the loading efficiency (Table 5). However, the increase in loading ratios subsided beyond pepsin concentrations of 5 mg/mL, while the specific activity of immobilized biocatalyst tends to decline.

In fact, the initial steep increases in enzymatic activity substantially slowed down for pepsin concentrations higher than 3 mg/mL despite the unceasing rise in load on support, which strongly suggests that the latest adsorbed bio-macromolecules tend to form a multilayered shell due to limited to none surface patches still available for direct adsorption on the nanoparticles. This behavior is strongly influenced by the physical strength of protein-protein interactions.[46,47] At the same time such interactions are modified upon adsorption on amino-functionalized surfaces due to the changes arisen in spatial distribution of polypeptide chains and charges.

The pepsin progressive distribution was substantially different in the case of multi-point covalent attachment with glutaraldehyde capped nanoparticles (MNp-Ga) and exhibited lower values of loading efficiency and specific activity. For example, a load of 0.82 mg /mg support along with a specific activity of 46.76 U/mg pepsin were obtained for pepsin concentrations of 4 mg/mL, both at about a half from those obtained at immobilization by adsorption in similar conditions. This fact could be explained by the longer distance from pepsin to the nanoparticle surface due to the glutaraldehyde spacer, different spatial conformation and flexibility of protein, and side reactions like covalent attachment of pepsin on more than one nanoparticle. Usually such processes cooperatively contribute to an effective reduction in availability and use of active support surfaces, leading to enzyme inactivation.

The kinetic parameters of free and immobilized pepsin

Based on the previous results, MNp-P (pepsin loading - 2.04 mg/mg) and MNp-Ga-P (pepsin loading - 0.82 mg/mg) samples have been selected for comparative determination of kinetic parameters. The proteolytic activity of free and immobilized enzyme was evaluated in similar experimental conditions (pH 2.0, 37ºC, 10 min) on hemoglobin solutions having initial concentrations in the range of 79.37-469.45 μM. The increase in hemoglobin concentration was accompanied by an intensification of the hydrolytic activity in all instances. As expected, pepsin has performed better in solution than under immobilized form, reaching an activity maximum of ~ 106.1 μM Tyr/min/mg at the highest concentration of hemoglobin (Figure 3).

However, the efficiency of MNp-P biocatalyst was just slightly lower in comparison with that of free pepsin, varying for different substrate concentrations between 87.8% and 89.7%, while the MNp-Ga-P activity was down to only 39.8%-44.1%. It must be also mentioned that activity of all samples, including free pepsin, tends to reach a plateau beyond substrate concentrations of around 380 μM, which strongly suggests the occurrence of an inhibition process regarding the formation of substrate-enzyme complex.[48] The kinetic constants of free and immobilized pepsin, V_{max} and K_m (Table 6), were determined based on the relationship between substrate concentration (S, μM) and enzymatic reaction rate (V, U/mg) described by Michaelis–Menten equation under Lineweaver–Burk linear graphic representation (1/V *versus* 1/S).

Table 5

Influence of the initial pepsin concentration on pepsin loading and activity

free pepsin (mg/mL)	loading efficiency (mg/mg support)	specific activity (U/mg pepsin)
2	0.69	58.26
3	1.05	81.57
4	1.40	84.05
5	2.04	95.72
6	2.25	93.86

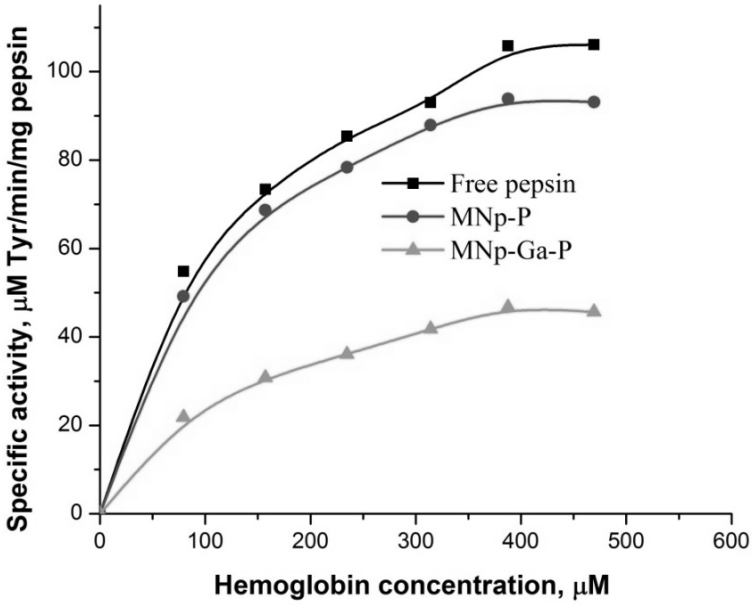

Fig. 3 – Effect of substrate concentration on the activities of free and immobilized pepsin.

Table 6

Kinetic parameters of free and immobilized pepsin

Biocatalyst type	V_{max} (μM/min/mg pepsin)	K_m (μM)	Catalytic efficiency (V_{max}/K_m)
Free pepsin	128.20	108.42	1.18
MNp-P	117.64	110.57	1.06
MNp-Ga-P	59.88	140.76	0.42

The V_{max} value for free pepsin was found to be more than 2 times higher than that obtained after covalent immobilization, indicating a severe decrease in the biocatalyst ability to convert a given amount of substrate in a time unit. Such decrease is accompanied by a milder reduction in the affinity for substrate, as shown by the comparatively lower increase in the apparent K_m value (1.27 times higher). At the same time, the physical adsorption involves a reduction of less than 10% in V_{max} and increases of just about 2% in the K_m value. These variations of kinetic parameters upon immobilization on the magnetite surfaces are mainly driven by the structural and morphological changes in the architecture of protein macromolecules, and by the lower accessibility of substrate to the active site of enzyme.[49] Similar tendencies were also reported in previous studies regarding the immobilization of different enzymes on silicone elastomers,[50] polymeric silicone material[51] and the aldehyde-modified polymethacrylate monolith.[28]

Reusability and storage stability

The operational stability and number of catalytic cycles achieved without a significant efficiency loss are very important from the applicative point of view, representing the main advantages of immobilized biocatalysts *versus* their free, soluble forms. The enzymatic activity was evaluated as previously described, by monitoring the tyrosine formation through hemoglobin hydrolysis in the presence of 1 mg immobilized pepsin. The reusability of MNp-P and MNp-Ga-P samples was tested at 37ºC by performing ten consecutive catalytic cycles. At the end of each cycle the used catalyst enzyme was magnetically separated, washed 3 times with HCl 0.01M and transferred to a fresh reaction medium.[31] The influence of recycling on the activity of pepsin immobilized samples is shown in Figure 4.

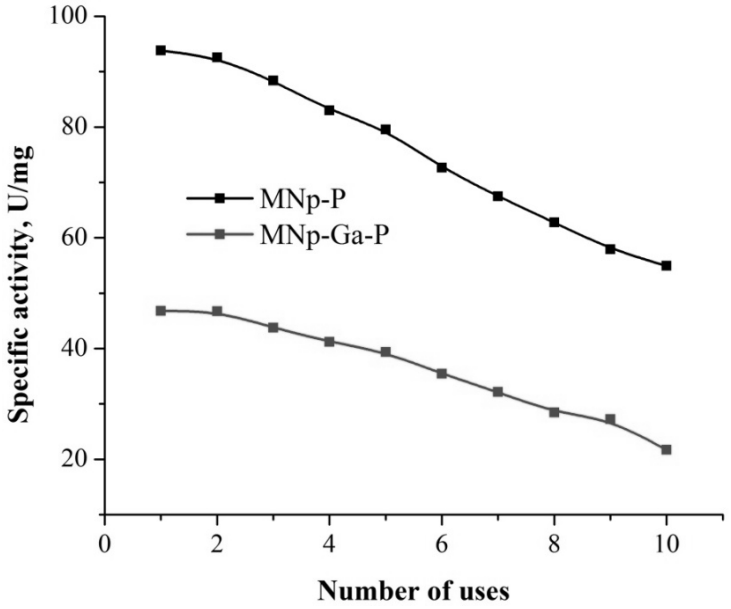

Fig. 4 – The reusability of immobilized pepsin.

Both immobilized biocatalysts have retained a specific activity of around 94% after three, and about 84-85% after five subsequent uses, which is high enough to justify the biocatalyst reusability from an applicative point of view [A-C]. Overall, the residual specific activity was on gradually and relative constant decrease beyond the second cycle, reaching 58.5% for the physical and 46.4% for the covalently bonded pepsin after ten cycles. After three months of storage at 4 ºC the proteolytic activity of pepsin immobilized through either technique has been kept at about 95-98% from the initial values while the activity of the free form dramatically decreased to only 8–10%.

EXPERIMENTAL

Materials

Pepsin from porcine gastric mucosa (EC 3.4.23.1; activity: ≥ 250 units/mg) and hemoglobin powder from bovine blood (~64.500 relative mass) suitable as protease substrate were products of Sigma-Aldrich. Reagent grade (3-aminopropyl)triethoxysilane (APTES), ferric chloride hexahydrate ($FeCl_3$ x $6H_2O$), ferrous chloride tetrahydrate ($FeCl_2$ x $4H_2O$), 4-nitrobenzaldehyde (4-NBA), ammonium hydroxide (28% v/v), glutaraldehyde (25% v/v), trichloroacetic acid (TCA), citric acid, acetic acid, ethanol, methanol, triethylamine, tyrosine were also obtained from Sigma-Aldrich. All materials were used as received and aqueous solutions were prepared with deionized water.

Synthesis of magnetite nanoparticles covered with citric acid MNp-CA

The two iron salts, ferric chloride hexahydrate $FeCl_3$ x $6H_2O$ (4.75 g, 17.57 mmol) and ferrous chloride tetrahydrate $FeCl_2$ x $4H_2O$ (1.74 g, 8.75 mmol) were dissolved in 100 mL previously degassed deionized water. The reaction mixture was stirred with an overhead mechanic stirrer (800 rmp), under a continuous flow of nitrogen at 80 °C. The reaction flask was equipped with an ascending condenser, followed by the rapid addition of 30 mL of ammonium hydroxide NH_4OH 28%. The reaction was continued for 24 h at 80 °C and a constant stirring speed of 800 rpm. The reaction flask was connected to a vacuum pump in order to remove the excess volatile ammonia NH_3. After 30 min, citric acid (approximately 7g) was added until the pH of the reaction mixture was slightly acidic (pH = 4-5 units). The stirring was continued for 24 h at 80 °C and 1000 rpm.

The reaction mixture was then cooled to room temperature, the particles were separated with a magnet and the supernatant discarded. The particles were washed repeatedly with deionized water (5x100 mL) and methanol (5x50 mL) using the same magnet to rapidly separate them, followed by drying under vacuum at 40 °C overnight.

Preparation of magnetite particles covered with (3-aminopropyl)silane MNp-APS

In order to ensure an adequate functionality for the immobilization of enzymes, the citric acid covered nanoparticles were subjected to a ligand exchange reaction,[52] when the citric acid on the nanoparticle surface is replaced with (3-aminopropyl)silane residues APS. In a typical experiment the citric acid particles (4 g) were dispersed in ethanol (70 mL) using an ultrasound bath. The (3-aminopropyl)triethoxysilane monomer (10 mL) was dissolved in absolute ethanol (25 mL) and added dropwise under a constant flow of nitrogen to the particle dispersion using a dropping funnel under continuous stirring (800 rmp). Following the complete addition of the silane solution triethylamine (3 mL) and water (1 mL) were added to catalyze the coupling reaction between the silane monomer and particles. The reaction flask was equipped with an ascending condenser and the reaction was continued for 24 h at 80 °C and a constant stirring speed (800 rpm). An aliquot from the reaction mixture was extracted and the particles were purified by washing with water (3x20 mL) and methanol (3x15 mL). The reaction mixture was supplied with an additional 2 mL of

APTES and the reaction was continued for 24 h at 80 °C and a constant stirring speed (800 rpm). The reaction flask was cooled to room temperature, the particles were decanted with a magnet and the colorless supernatant discarded. The particles were then washed successively with water (5x100 mL) and methanol (3x50 mL), followed by drying under vacuum at 40°C overnight.

Surface immobilization of pepsin

In the case of pepsin immobilization by physical adsorption the magnetite nanoparticles were used as synthesized, without any subsequent surface modification. Pepsin solutions of various concentrations have been prepared in 0.01 M HCl (pH 2.0) to maintain the enzymatic activity and prevent denaturation. Freshly prepared pepsin solutions (20 mL) were added to dry MNp (25 mg) in Erlenmeyer flasks and incubated at 4ºC for 24 h, under a stirring just strong enough to maintain a colloidal suspension. The resulting biocatalytic nanoparticles (MNp-P) were separated from suspension by using an external magnet and washed with 0.01M HCl several times, until pepsin becomes undetectable in the washing solutions. The overall pepsin concentrations in supernatant and washing solutions (C_f) were determined by reading their absorbances at 280 nm and interpolate them within a calibration curve plotted with pepsin solutions of known concentrations.[27] Protein loading (P) onto MNp-APS surface (mg/mg) was quantified with the formula:

$$P = (C_i - C_f) / M \quad (1)$$

where C_i and C_f represent the initial and final amounts of solubilized pepsin, and M the solution content in suspended MNp (mg).

The covalent immobilization of pepsin was achieved with a multi-step technique. A glutaraldehyde solution (1.5 mL, 25%) was poured into an amino functionalized magnetite suspension (30 mL, 1mg/mL) and reacted for 4 h at 250 rpm and 37ºC. After magnetic separation and several washes with deionized water, the surface-modified MNp were re-suspended in 20 mL pepsin solution (4 mg/mL, pH 2.0) and incubated for 5 h in the same experimental conditions that were set for physical adsorption.[53] The glutaraldehyde linked biocatalytic nanostructures (MNp-Ga-P) obtained in the second stage were furthermore extracted from suspension by magnetic separation and washed with 0.01 M HCl solutions (pH 2.0) until the complete elimination of unbounded pepsin. The amounts of free and immobilized protein have been determined as previously described, based on the values of pepsin absorbance from 280 nm. In order to better stabilize the covalent attachment of enzyme, the crude MNp-Ga-P assemblies were finally treated with sodium cyanoborohydride (5 mL, 0.1M) for 2h, magnetically separated and washed again several times. The immobilized pepsin was dried and stored at 4ºC until use.

Methods

Fourier transform infrared (FT-IR) spectra were measured on a FTIR Bruker Vertex 70 spectrophotometer, in transmission mode, using KBr pellets.

Elemental analysis. Determinations of the elemental composition have been carried out using a scanning electron microscope Quanta 200, equipped with an energy-dispersive X-ray (EDX) detector. The solid samples were placed on double-sided carbon tape mounted on aluminum stubs. The weight percentage (wt%) and atomic percentage (at%) concentrations of the elements in the samples were determined.

Electron Microscopy. The size and shape of produced nanoparticles were evaluated using a Hitachi HT7700 transmission electron microscope at 100 kV in High Resolution Mode. The samples were dispersed by ultrasonication in water and one drop of this solution was placed on a carbon-coated grid leaving the solvent to evaporate in an oven at 40°C for 72 hours before analysis.

Particle size and zeta potential measurements. Particle size and Zeta potential measurements were performed on a Delsa Nano C Submicron Particle Size Analyzer (Beckman Coulter, Inc., Fullerton, CA), equipped with a laser diode operating at 658 nm. The nanoparticles solutions were dispersed by ultrasonication and size and Zeta measurements were measured in Flow Cell at room temperature.

UV-VIS measurements. The quantification of enzyme and tyrosine concentrations was carried out by reading the absorbance of solution at 280 nm by using standard 1 cm quartz cuvettes and a LAMBDA 35 (Perkin Elmer) UV-Vis spectrophotometer.

Quantification of amino groups on the surface of MNp-APS. Four samples of MNp-APS with progressive quantities (25, 50, 75 and 100 mg) were incubated with 3 mL of a 4-nitrobenzaldehyde 0.02 M methanol solution for 4 h at 50 °C. The excess solution of 4-NBA was then removed and the decanted particles were washed with ethanol (10 mL) and methanol (10 mL) The dried particles were then redispersed in 3 mL deionized water containing 20 µL acetic acid, followed by incubation for 15 h at 50 °C in order to hydrolyze the 4-NBA from the formed Schiff base. The acid cleaved aldehyde is then measured spectrophotometrically at 267 nm and quantified using a calibration curve. The released 4-nitrobenzaldehyde is proportional to the number of amino groups available on the surface of the APTES covered particles. The calibration curve was obtained by the representation of the absorbance intensity measured at 267 nm (specific to 4-NBA) *versus* the concentration of 4-NBA solution in the 0.335-4.69 µg/mL range.

The proteolytic activity of free and immobilized pepsin. The activity of free and immobilized enzyme was evaluated according to a slightly modified Bisswanger method, based on the quantification of tyrosine amount released from the hydrolysis of hemoglobin.[54] Either 0.1 ml pepsin solutions (5 mg/mL, pH 2.0) or corresponding amounts of MNp-P (pepsin load of 2.04 mg/mg) or MNp-Ga-P (pepsin load of 0.82 mg/mg) biocatalysts were added into test tubes containing 0.5 mL hemoglobin (25 mg/mL, pH 2.0). The hemoglobin solutions were previously incubated at 37°C, 300 rpm for 5 minutes. All reactions were stopped after 10 minutes by addition of 1 mL TCA (5%, w/v). In the case of immobilized pepsin the nanoparticles were removed by magnetic separation just before denaturation. The resulting precipitate was stirred for another 5 minutes and centrifuged at 5000g for 10 minutes. The supernatant absorbance at 280 nm is proportional with the amount of low molecular weight hydrolyzed products soluble in TCA, expressed as tyrosine equivalents. Blank samples, with pepsin added to similar concentrations of hemoglobin after denaturation with TCA, were also prepared and absorbance values subtracted from the sample ones. The amounts of released tyrosine were obtained from a standard tyrosine curve, which show excellent linearity for the concentration between 54.50 - 545.00 µM. In these experimental conditions, one unit (U) of enzymatic activity at hemoglobin hydrolysis was defined as the amount of tyrosine (µM) released in solution per minute at 37°C, pH=2, by 1 mg free or immobilized pepsin.[25] The kinetic parameters for both free and immobilized pepsin (Michaelis constant, K_m; maximum rate, V_{max}) and catalyst efficiency values were determined in the same experimental conditions (37ºC,

pH=2, 10 min reaction time) for substrate concentrations varying in the range of 79.37-469.45 μM, by using Lineweaver–Burk plots.

CONCLUSIONS

Silanized core-shell magnetite nanoparticles with a relative spherical shape and a mean diameter of about 15-20 nm have been successfully synthesized through a reproducible and efficient two-step method. Their surface functionalization with amino groups has furthermore conduct to a new proper support for pepsin immobilization by either covalent linking or physical interaction, which was confirmed by FT-IR, EDX, TEM and DLS analyses. A maximum immobilization degree of 2 mg pepsin/1 mg magnetic nanoparticles was achieved in optimum conditions. It was also confirmed that the synthesized magnetite-pepsin constructs are catalytically active and have the capacity to catalyze several cycles of hemoglobin hydrolysis after successive recoveries through magnetic separation. Thus, it can be concluded that these biocatalytical active products are also reusable, which is very important from the applicative point of view. Moreover, the resistance of obtained biocatalysts in acidic environments, alongside with the possibility of rapid magnetic separation from protein hydrolysate solutions, allows their use in microfluidic devices for the identification and separation of different biomolecules from biological samples.

Acknowledgements. This publication is part of a project that has received funding from the European Union's Horizon 2020 research and innovation program under the grant agreement No. 667387 WIDESPREAD 2-2014 SupraChem Lab. This work was also supported by a grant of the Roumanian National Authority for Scientific Research and Innovation, CNCS/CCCDI – UEFISCDI, project number PN-III-P3-3.6-H2020- 2016-0011, within PNCDI III.

REFERENCES

1. A. Liese and L. Hilterhaus, *Chem. Soc. Rev*., **2013**, *42*, 6236-6249.
2. E. L. Ticu, D. Vercaigne-Marko, R. Froidevaux, A. Huma, V. Artenie and D. Guillochon, *Process Biochem*, **2005**, *40*, 2841-2848.
3. C. Mateo, J. M. Palomo, G. Fernandez-Lorente, JM. Guisan and R. Fernandez-Lafuente, *Enzyme Microb. Technol.*, **2007**, *40*, 1451-1463.
4. L. Cao, "Adsorption-based Immobilization", in "Carrier-bound Immobilized Enzymes", L. Cao (Ed.), Wiley, 2005, p. 53-168.
5. T. Jesionowski, J. Zdarta and B. Krajewska, *Adsorption*, **2014**, *20*, 801-821.
6. P. Zucca and E. Sanjust, *Molecules,* **2014**, *19*, 14139-14194.
7. L. Cao, "Covalent Enzyme Immobilization", in "Carrier-bound Immobilized Enzymes", L. Cao (Ed.), Wiley, 2005, p. 169-316.
8. Q. Husain, *Crit. Rev. Biotechnol.,* **2010**, 30, 41-62.
9. L. M. Rossi, N. J. S. Costa, F. P. Silva and R. Wojcieszak, *Green Chem.*, **2014**, *16*, 2906-2933.
10. M. J. Jacinto, F. P. Silva, P. K. Kiyohara, R. Landers and L. M. Rossi, *ChemCatChem*, **2012**, *4*, 698-703.
11. A. Durdureanu-Angheluta, M. Pinteala and B.C. Simionescu, "Tailored and functionalized magnetite particles for biomedical and industrial applications", in "Materials Science and Technology", S. D. Hutagalung (Ed), InTech, 2012, p. 149-179.
12. E. van Leemputten and M. Horisberger, *Biotechnol. Bioeng.*, **1974**, *16*, 385-396.
13. P. A. Johnson, H. J. Park and A. J. Driscoll, "Enzyme Nanoparticle Fabrication: Magnetic Nanoparticle Synthesis and Enzyme Immobilization", in "Enzyme Stabilization and Immobilization. Methods in Molecular Biology (Methods and Protocols)", vol. 679, S. Minteer (Ed), Humana Press, 2011, p. 183-191.
14. H. Vaghari, H. Jafarizadeh-Malmiri, M. Mohammadlou, A. Berenjian, N. Anarjan, N. Jafari and S. Nasiri, *Biotechnol. Lett.*, **2016**, *38*, 223-233.
15. W. Jiang, K. L. Lai, H. Hu, X. B. Zeng, F. Lan, K. X. Liu, Y. Wu and Z. W. Gu, *J. Nanopart. Res.,* **2011**, *13*, 5135-5145.
16. T. P. Almeida, T. Kasama, A. R. Muxworthy, W. Williams, L. Nagy, T. W. Hansen, P. D. Brown and R. E. Dunin-Borkowski, *Nat. Commun.*, **2014**, *5*, 5154-5160.
17. R. Valenzuela, M. C. Fuentes, C. Parra, J. Baeza, N. Duran, S. K. Sharma, M. Knobel and J. Freer, *J. Alloys Comp.*, **2009**, *488*, 227-231.
18. S. Rani and G. D. Varma, *Physica B Condens. Matter.*, **2015**, *472*, 66-77.
19. M. Szekeres, I. Y. Tóth, E. Illés, A. Hajdú, I. Zupkó, K. Farkas, G. Oszlánczi, L. Tiszlavicz and E. Tombácz, *Int. J. Mol. Sci.*, **2013**, *14*, 14550-14574.
20. L. Li, K. Y. Mak, C. W. Leung, K. Y. Chan, W. K. Chan, W. Zhong and P. W. T. Pong, *Microelectron. Eng.*, **2013**, *110*, 329-334.
21. F. Horst, E. H. Rueda and M. L. Ferreira, *Enzyme Microb. Tech.*, **2006**, *38*, 1005-1012.
22. L. J. Daumann, J. A. Larrabee, D. Ollis, G. Schenk and L. R. Gahan, *J. Inorg. Biochem.*, **2014**, *131*, 1-7.
23. M. F. C. Andrade, A. L. A. Parussulo, C. G. C. M. Netto, L. H. Andrade and H. E. Toma, *Biofuel Res. J.*, **2016**, *10*, 403-409.
24. V. K. Antonov, L. M. Ginodman, Y. V. Kapitannikov, T. N. Barshevskaya, A. G. Gurova and L. D. Rumsh, *FEBS Lett.*, **1978**, *88*, 87-90.
25. G. D. Altun and S. A. Cetinus, *Food Chem.*, **2007**, *100*, 964-971.
26. J. Frýdlová, Z. Kučerová and M. Tichá, *J. Chromatogr. B*, **2004**, *800*, 109-114.
27. D. Meridor and A. Gedanken, *Enzyme Microb. Tech.*, **2014**, *67*, 67-76.
28. W. Han, M. Yamauchi, U. Hasegawa, M. Noda, K. Fukui, A. J. van der Vlies, S. Uchiyama and H. Uyama, *J. Biosci. Bioeng.,* **2015**, *119*, 505-510.
29. J. Li, J. Wang, V. G. Gavalas, D. A. Atwood and L. G. Bachas, *Nano Letters*, **2003**, *3(1)*, 55-58.
30. M. Höldrich, A. Sievers-Engler and M. Lämmerhofer, *Anal. Bioanal. Chem.*, **2016**, *408*, 5415-5427.

31. H. M. Kayili and B. Salih, *Talanta*, **2016**, *155*, 78-86.
32. M. M. Lakouraj, A. Maashsani, R. S. Norouzian and M. Mohadjerani, *J. Carbohyd. Chem.*, **2015**, *34*, 103-119.
33. A. Bandhu, S. Sutradhar, S. Mukherjee, J. M. Greneche and P. K. Chakrabarti, *Mat. Res. Bull.*, **2015**, *70*, 145-154.
34. A. Durdureanu-Angheluta, L. Pricop, I. Stoica, C. A. Peptu, A. Dascalu, N. Marangoci, F.Doroftei, H.Chiriac, M.Pinteala and B. C.Simionescu, *J. Magn. Magn. Mater.*, **2010**, *322*, 2956-2968.
35. J.L. Zhang, R.S. Srivstava and R.D.K. Misra, *Langmuir*, **2007**, *23*, 6342–6351.
36. R. Fu, W. Wang, R. Han and K. Chen, *Mater Lett*, **2008**, *62*, 4066–4068.
37. A. Durdureanu-Angheluta, C. Mihesan, F. Doroftei, A. Dascalu, L. Ursu, M. Velegrakis and M. Pinteala, *Rev. Roum. Chim.*, **2014**, *59*, 151–159.
38. A. Durdureanu-Angheluta, A. Dascalu, A. Fifere, A. Coroaba, L. Pricop, H. Chiriac, V. Tura, M. Pinteala and B.C. Simionescu, *J Magn Magn Mater*, **2012**, *324*, 1679–1689.
39. A. Gole, C. Dash, V. Ramakrishnan, S. R. Sainka,r A. B. Mandale, M. Rao and M. Sastry, *Langmuir*, **2001**, *17*, 1674–1679.
40. J. Tang, P. Sepulveda, J. Marciniszyn, Jr., K. C. S. Chen, W-Y. Huang, N. Tao, D. Liu and J. P. Lanier, *Proc. Natl. Acad. Sci. U S A*, **1973**, *70*, 3437–3439.
41. S. Bhattacharjee, *J. Control. Release*, **2016**, *235*, 337–351.
42. J.H. Moon, J.H. Kim, K.J. Kim, T.H. Kang, B. Kim, C.H. Kim, J.H. Hahn and J.W. Park, *Langmuir*, **1997**, *13*, 4305–4310.
43. A. Abbas, C. Vivien, B. Bocquet, D. Guillochon and P. Supiot, *Plasma Process. Polym.*, **2009**, *6*, 593–604.
44. A. Chiriac, L. E. Nita, S. Cimmino, C. Silvestre and D. Duraccio, *J. Optoelectron. Adv. Mater.,* **2007**, *9*, 3431 – 3434.
45. X.-D. Tong, B. Xue and Y. Sun, *Biotechnol. Prog.,* **2001**, *17*, 134–139.
46. Y. Sui, Y. Cui, Y. Nie, G.M. Xia, G.X. Sun and J.T. Han, *Colloid Surf. B*, **2012**, *93*, 24–28.
47. G. Bayramoglu, B. Kaya and M.Y. Arıca, *Food Chem.,* **2005**, *92*, 261–268.
48. T.K. Ozturk and A. Kilinc, *J. Mol. Catal. B: Enzym.,* **2010**, *67*, 214–218.
49. J.F. Kennedy, E.H.M. Melo and K. Jumel, *Chem. Eng. Prog*. **1990**, *86*, 81–89.
50. Y. Poojari, A.S. Palsule, S.J. Clarson and R.A. Gross, *Silicon*, **2009**, *1*, 37–45.
51. A. Durdureanu-Angheluta, M-E Ignat, S.S. Maier, L. Pricop, A. Coroaba, A. Fifere, M. Pinteala and A. Chiriac, *Appl. Surf. Sci.*, **2014**, *292*, 898–905.
52. R. D. Palma, S. Peeters, M. J. V. Bael, H. V. d. Rul, K. Bonroy, W. Laureyn, J. Mullens, G. Borghs and G. Maes, *Chem. Mater.,* **2007**, *19*, 1821–1831.
53. S. Kumar, A.K. Jana, I. Dhamija, Y. Singla and M. Maiti, *Eur J Pharm Biopharm*, **2013**, *85*, 413–426.
54. H. Bisswanger, "Practical enzymology", Wiley-VCH, Weinheim, Germany, 2004, p. 140–141.